

## Supplementary information

for

# Light-induced pulling and pushing by synergic effect of optical force and photophoretic force

Jinsheng Lu, Hangbo Yang, Lina Zhou, Yuanqing Yang, Si Luo, Qiang Li and Min Qiu

State Key Laboratory of Modern Optical Instrumentation, College of Optical Science and

Engineering, Zhejiang University, 310027, Hangzhou, China

E-mail: [minqiu@zju.edu.cn](mailto:minqiu@zju.edu.cn)

## Contents

13	1 Tapered fiber fabrication and micrometer-sized gold plate synthesis.....	2
14	2 Experimental procedures of optical driving.....	2
15	3 Theoretical calculation of total electromagnetic force for the supercontinuum light.....	3
16	4 Temperature and photophoretic force calculations.....	5
17	5 Optical pulling force analysis using Maxwell stress tensor decomposition method.....	9
18	6 Optical force perpendicular to the gold plate surface .....	13
19	7 Force analysis from gold plate movements in experiment.....	14
20	References .....	16

23    **1 Tapered fiber fabrication and micrometer-sized gold plate synthesis**

24    The tapered fiber is fabricated using a flame-heated drawing technique [1]. The fabrication  
25    procedures can be described as follows: A certain region of coating layer of a single mode  
26    optical fiber is removed. Put the prefabricated fiber on the flame of alcohol blast burner and  
27    pull the fiber quickly when it begins to melt until the two sections of the fiber is separated. A  
28    tapered fiber is then fabricated. The diameter of tapered fiber tip can reach to sub-micrometer.  
29    The gold plate used here is synthesized in a mixture of chloroauric acid ( $\text{AuCl}_3 \cdot \text{HCl} \cdot 4\text{H}_2\text{O}$ )  
30    and aniline ( $\text{C}_6\text{H}_7\text{N}$ ) as reported previously [2]. The side length and thickness of synthesized  
31    gold plate is several micrometer to a dozen micrometer and dozens of nanometer respectively.  
32    The cone angle of the tapered fiber used is about  $6^\circ$  and the gold plate is with side length 5.4  
33     $\mu\text{m}$  and thickness 30 nm in this experiment.

34    **2 Experimental procedures of optical driving**

35    The supercontinuum light source is a SuperK COMPACT supercontinuum laser (bandwidth,  
36    450 nm~2,400 nm; unpolarized). The light is delivered to a single mode fiber and connected  
37    to a tapered fiber with a standard FC/PC connector. The total power of the light guided into  
38    the tapered fiber is 1.3 mW. The gold plates are deposited on the glass substrate and then  
39    dried. The tapered fiber is manipulated by the three dimensional console to pick up the gold  
40    plate indicated with a white arrow in Fig. S1a. The tapered fiber with the gold plate on the tip  
41    is lifted up above the substrate in air and as expected the other gold plates on the substrate are  
42    defocused in Fig. S1c (as compared to Fig. S1b). Finally after turning on the supercontinuum  
43    light, we can see that the gold plate are pulled and pushed optically through the camera

44 controlled by a computer.



45

46 **Figure S1 | Experimental procedures.**

47 **3 Theoretical calculation of total electromagnetic force for the supercontinuum light**

48 Here, we use the commercial software *FDTD solutions* (v8.13, Lumerical) to calculate the  
49 electric and magnetic field distributions with 3D simulations. The optical force of single  
50 wavelength light source then is calculated using Maxwell Stress Tensor (MST) method [3].  
51 Although the gap between the gold plate and the tapered fiber is unknown for us in the  
52 experiment, we choose the gap as 50 nm in all simulations according to the Debye length  
53 which is usually used in calculations for the typical length in the electrostatic interaction [4,  
54 5]. The supercontinuum light induced optical force is derived from the overlap integral  
55 between single-wavelength light-induced optical force spectrum and light source power  
56 density spectrum.

57 In order to model the tapered fiber in simulation, we polyfit the contour of the optical  
58 microscopy image of tapered fiber  $C(x)$  with the function (suppose that the tapered fiber is  
59 rotational symmetry):

$$C(x) = -0.0642 \cdot x^6 + 0.7550 \cdot x^4 + 6.8994 \cdot x^2 - 1.4137 \quad (\text{S1})$$

60 We use a grid size ( $dx$ , 30 nm;  $dy$ , 10nm;  $dz$ , 30 nm) for the gold plate-tapered fiber structure.  
61 In order to appropriately reduce both the simulation memory and simulation time, we have

62 tuned the grid size in simulation and find this value is enough in the accuracy for the optical  
 63 force calculation. The bandwidth of supercontinuum light source is 450 nm ~ 2,400 nm. Here  
 64 we have calculated 21 wavelengths with an interval of 97.5 nm. The electric field amplitude  
 65 of the mode source is set as 1 V/m.

66 Further, the total optical force of supercontinuum light source can be calculated by  
 67 integrating the optical force of single wavelength with the spectra  $P(\lambda)$  of the light source in  
 68 Fig. S2. The total optical force can be calculated as follows:

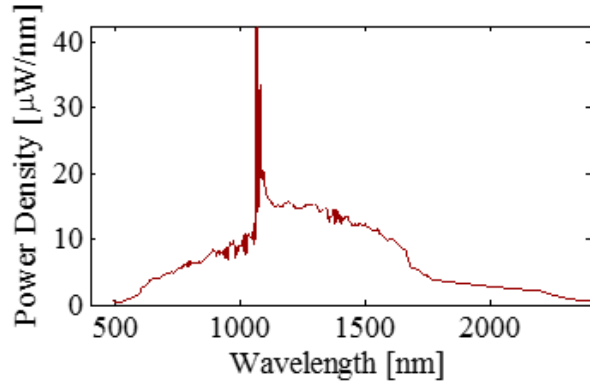
$$P_\lambda = \frac{1}{2} \pi W_\lambda^2 I_\lambda = \frac{1}{2} \pi W_\lambda^2 \sqrt{\epsilon_0 / \mu_0} |A_\lambda|^2 \Rightarrow |A_\lambda|^2 = \frac{2\sqrt{\mu_0 / \epsilon_0} P_\lambda}{\pi W_\lambda^2}$$

$$F_\lambda \propto |A_\lambda|^2, |A_\lambda| = 1 \rightarrow F_{\lambda,0} \Rightarrow F_\lambda = F_{\lambda,0} |A_\lambda|^2 = F_{\lambda,0} \frac{2\sqrt{\mu_0 / \epsilon_0} P_\lambda}{\pi W_{\lambda,0}^2}$$

$$F_{total} = \sum_i^N (F_{\lambda_i,0} \frac{2\sqrt{\mu_0 / \epsilon_0} M_{\lambda_i} B / N}{\pi W_{\lambda_i,0}^2})$$

69 where  $\epsilon_0 = 8.854 \times 10^{-12}$  F·m<sup>-1</sup> is the vacuum permittivity and  $\mu_0 = 1.257 \times 10^{-6}$  H·m<sup>-1</sup> is the  
 70 permeability constant.  $|A_\lambda|$  is the amplitude of electric filed at the center of mode source  
 71 with wavelength  $\lambda$  and  $W_\lambda$  is the mode source waist radius.  $P_\lambda$  is the power of the mode  
 72 source.  $M_{\lambda_i}$  is the power density of the broadband light source.  $F_{\lambda,0}$  is the calculated optical  
 73 force when the wavelength is  $\lambda$  and the electric field amplitude of mode source is 1 V/m.  $B$  is  
 74 the bandwidth of the light source. The bandwidth is divided into  $N$  infinitesimal element  $\Delta\lambda$ .  
 75 The larger  $N$  is, the more accurate the result will be. (In our simulation:  $N$ , 21;  $B$ , 1950 nm;  
 76  $\Delta\lambda$ , 97.5 nm.)

77

78 **Figure S2 | Spectra of the supercontinuum light in the tapered fiber.**79 **4 Temperature and photophoretic force calculations**80 **4.1 Temperature calculations methods**

81 From the FDTD results, the electric field distribution in the gold plate can be extracted and  
 82 the heat power volume density  $Q_d(x, y, z, \lambda)$  can be calculated as [6]

$$Q_d(x, y, z, \lambda) = \frac{1}{2} \varepsilon_0 \omega \text{Im}(\varepsilon_r) |\mathbf{E}(x, y, z, \lambda)|^2 \quad (\text{S3})$$

83 The supercontinuum light induced heat power volume density  $Q_d(x, y, z)$  is derived from  
 84 overlap integral between the single wavelength light induced heat power volume density  
 85 spectrum  $Q_d(x, y, z, \lambda)$  and the supercontinuum light source power density spectrum  $P(\lambda)$ .

$$Q_d(x, y, z) = \int Q_d(x, y, z, \lambda) \cdot P(\lambda) d\lambda \quad (\text{S4})$$

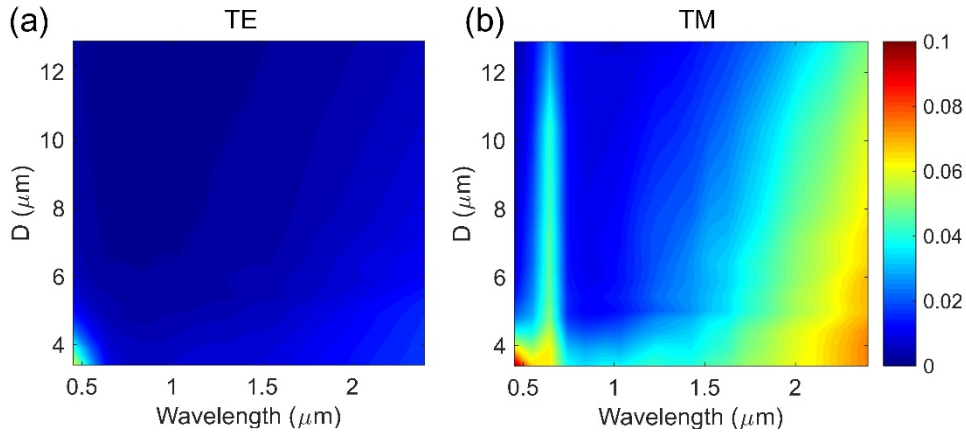
86 The temperature distribution of the tapered fiber-gold plate system is then calculated with  
 87 COMSOL Multiphysics using the calculated  $Q_d(x, y, z)$  as input.

88 **4.2 Wavelength-dependent absorption of the gold plate**

89 The absorptance of the gold plate in the configuration can be calculated with volumetric  
 90 integral of the heat power volume density  $Q_d(x, y, z, \lambda)$  dividing by the power of the source  
 91  $P_{source}$  as follows

$$A(\lambda) = \frac{\iiint Q_d(x, y, z, \lambda) dx dy dz}{P_{source}} \quad (S5)$$

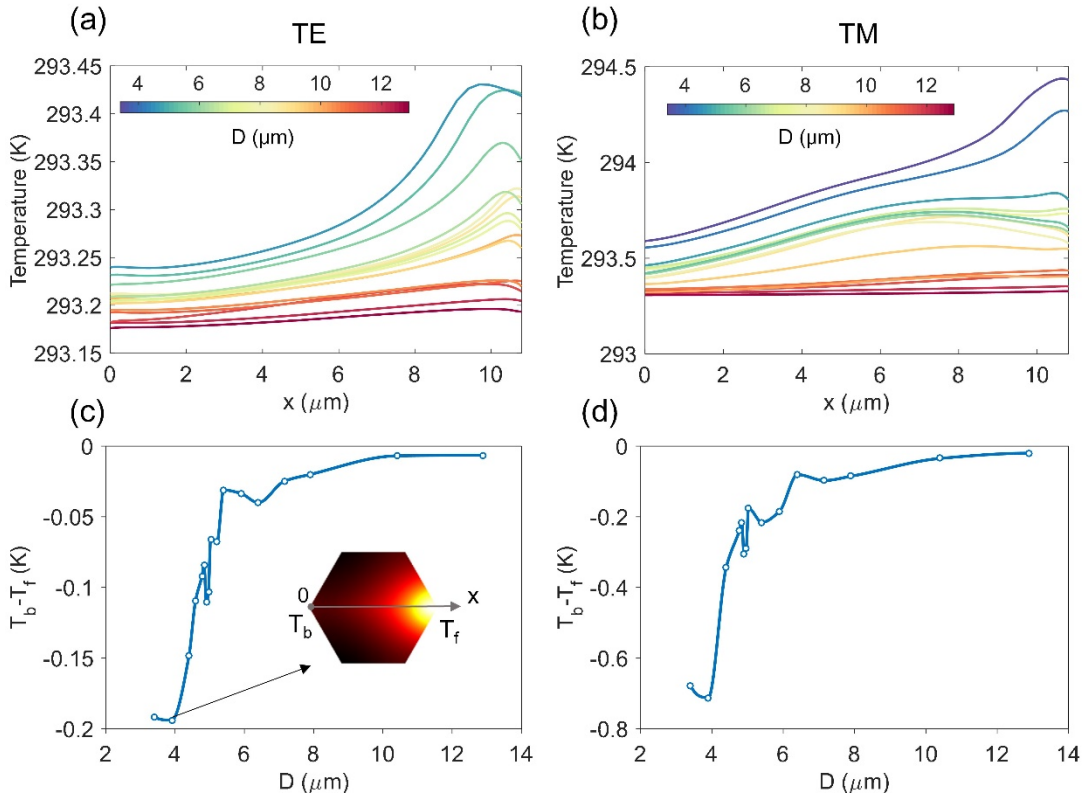
92 The absorptance of the gold plate changes with the position of the gold plate on the tapered  
 93 fiber and the wavelength of the source as Fig. S3 shows.



94  
 95 **Figure S3 | Calculated spectra of absorptance of the gold plate.** (a) TE mode. (b) TM  
 96 mode. The distance between the center of the gold plate and the tapered fiber end is D.

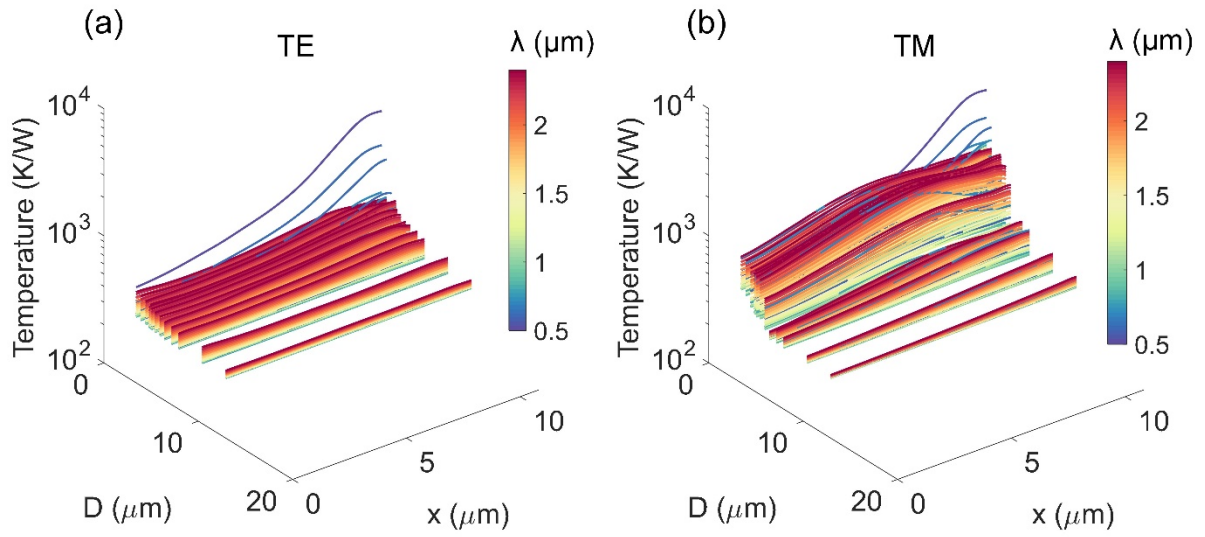
#### 97 **4.3 Temperature distribution and photophoretic force calculations**

98 The temperature line distribution on the surface of the gold plate from the back-end part ( $x=0$   
 99  $\mu\text{m}$ ) to the front part ( $x=10.8 \mu\text{m}$ ) is shown in Figs. S4(a,b). The temperature at the front part  
 100 of the gold plate is higher than that of the back-end part. With the location of the gold plate  
 101 being away from the tapered fiber end (i.e.,  $D$  increased), this difference goes to zero. The  
 102 temperature difference between the back-end part and the front part is shown as Figs. S4(c,d).



103

104 **Figure S4 | Temperature distribution of the gold plate.** (a, b) Temperature line distribution  
 105 along the gold plate from the back-end part to the front part (see the inset in (c) for the  
 106 x-coordinate) for (a) TE mode and (b) TM mode with respect to the distance ( $D$ ) between the  
 107 center of gold plate and the tapered fiber end. (c, d) Temperature difference ( $T_b - T_f$ ) changes  
 108 with respect to the location of the gold plate for (c) TE mode and (d) TM mode. The  
 109 temperature at back-end part and front part of the gold plate is  $T_b$  and  $T_f$  respectively. The  
 110 inset in (c) is the temperature distribution on the surface of the gold plate for  $D=3.9 \mu\text{m}$ .  
 111  
 112 In order to investigate the wavelength dependence of the photophoretic force, temperature  
 113 distribution of the gold plate for every single wavelength ( $\lambda$ ) of light source and different  
 114 distance ( $D$ ) between the center of gold plate and the tapered fiber end has been calculated as  
 115 shown in Fig. S5.  
 116



117  
118 **Figure S5 | Temperature distribution of the gold plate for different wavelength ( $\lambda$ ) of**  
119 **light source and different distance (D) between the center of gold plate and the tapered**  
120 **fiber end.** (a, b) Temperature line distribution along the gold plate from the back-end part  
121 (x=0) to the front part (x=10.8  $\mu\text{m}$ ) for (a) TE mode and (b) TM mode.

122  
123 Photophoretic force can be calculated using formula  $F^{PPF} = -15/(64\sqrt{2})k_B/\sigma_{cs} \cdot \alpha \cdot dT/dx \cdot S_v$   
124 [7-9]. Here,  $k_B = 1.38 \times 10^{-23} \text{ J}\cdot\text{K}^{-1}$ ; the scattering cross section of air molecules at 1 atm and  
125 room temperature is  $\sigma_{cs} = \pi \times (0.37 \text{ nm})^2 = 4.3 \times 10^{-19} \text{ m}^2$ ; the thermal accommodation coefficient  
126  $\alpha$  at T=300 K is about 0.8~0.9 [10], here we take  $\alpha=0.8$ ; the size along the temperature  
127 gradient is  $dx=10.8 \mu\text{m}$ ; since the average radius of the tapered fiber within the scope of our  
128 calculation is about 1.2  $\mu\text{m}$ , the active thermal creep flow region in the surface of the gold  
129 plate on the tapered fiber can be estimated as  $1.2 \mu\text{m} \times 10.8 \mu\text{m} = 12.96 \mu\text{m}^2$ . With the  
130 temperature difference calculated in Figs. S4(c,d), the photophoretic force then can be  
131 calculated as shown in Fig. 1(c) in the main text.

132    **5 Optical pulling force analysis using Maxwell stress tensor decomposition method**

133    **5.1 Decomposition of Maxwell stress tensor**

134    In order to investigate the optical force coming from which components of electromagnetic  
135    field, we decompose the Maxwell stress tensor to the get optical force as follows:

136    From [3, 5]

$$\mathbf{f}_j = \sum_i \nabla_i \cdot \overset{\text{t}}{\mathbf{T}}_{ij} \mathbf{e}_j \quad (\text{S6})$$

137    With  $\overset{\text{t}}{\mathbf{T}}_{ij} = \epsilon_0 \mathbf{E}_i \mathbf{E}_j + \mu_0 \mathbf{H}_i \mathbf{H}_j - \frac{\epsilon_0 \mathbf{E}^2 + \mu_0 \mathbf{H}^2}{2} \delta_{ij}$ , we obtain

$$\begin{aligned} f_x &= \frac{\partial}{\partial x} \overset{\text{t}}{\mathbf{T}}_{11} + \frac{\partial}{\partial y} \overset{\text{t}}{\mathbf{T}}_{21} + \frac{\partial}{\partial z} \overset{\text{t}}{\mathbf{T}}_{31} \\ f_x &= \frac{\epsilon_0}{2} \frac{\partial}{\partial x} (E_x^2 - E_y^2 - E_z^2) + \frac{\mu_0}{2} \frac{\partial}{\partial x} (H_x^2 - H_y^2 - H_z^2) \\ &\quad + \epsilon_0 \frac{\partial}{\partial y} (E_x E_y) + \mu_0 \frac{\partial}{\partial y} (H_x H_y) + \epsilon_0 \frac{\partial}{\partial z} (E_x E_z) + \mu_0 \frac{\partial}{\partial z} (H_x H_z) \end{aligned} \quad (\text{S7})$$

$$\begin{aligned} f_y &= \frac{\partial}{\partial x} \overset{\text{t}}{\mathbf{T}}_{12} + \frac{\partial}{\partial y} \overset{\text{t}}{\mathbf{T}}_{22} + \frac{\partial}{\partial z} \overset{\text{t}}{\mathbf{T}}_{32} \\ f_y &= \frac{\epsilon_0}{2} \frac{\partial}{\partial y} (E_y^2 - E_x^2 - E_z^2) + \frac{\mu_0}{2} \frac{\partial}{\partial y} (H_y^2 - H_x^2 - H_z^2) \\ &\quad + \epsilon_0 \frac{\partial}{\partial x} (E_x E_y) + \mu_0 \frac{\partial}{\partial x} (H_x H_y) + \epsilon_0 \frac{\partial}{\partial z} (E_y E_z) + \mu_0 \frac{\partial}{\partial z} (H_y H_z) \end{aligned} \quad (\text{S8})$$

$$\begin{aligned} f_z &= \frac{\partial}{\partial x} \overset{\text{t}}{\mathbf{T}}_{13} + \frac{\partial}{\partial y} \overset{\text{t}}{\mathbf{T}}_{23} + \frac{\partial}{\partial z} \overset{\text{t}}{\mathbf{T}}_{33} \\ f_z &= \frac{\epsilon_0}{2} \frac{\partial}{\partial z} (E_z^2 - E_x^2 - E_y^2) + \frac{\mu_0}{2} \frac{\partial}{\partial z} (H_z^2 - H_x^2 - H_y^2) \\ &\quad + \epsilon_0 \frac{\partial}{\partial x} (E_x E_z) + \mu_0 \frac{\partial}{\partial x} (H_x H_z) + \epsilon_0 \frac{\partial}{\partial y} (E_y E_z) + \mu_0 \frac{\partial}{\partial y} (H_y H_z) \end{aligned} \quad (\text{S9})$$

138    After a time average of the optical force density, we get

$$\begin{aligned} \langle f_x \rangle &= \frac{\epsilon_0}{4} \frac{\partial}{\partial x} (|E_x|^2 - |E_y|^2 - |E_z|^2) + \frac{\mu_0}{4} \frac{\partial}{\partial x} (|H_x|^2 - |H_y|^2 - |H_z|^2) \\ &\quad + \frac{\epsilon_0}{2} \frac{\partial}{\partial y} \operatorname{Re}(E_x E_y^*) + \frac{\mu_0}{2} \frac{\partial}{\partial y} \operatorname{Re}(H_x H_y^*) + \frac{\epsilon_0}{2} \frac{\partial}{\partial z} \operatorname{Re}(E_x E_z^*) + \frac{\mu_0}{2} \frac{\partial}{\partial z} \operatorname{Re}(H_x H_z^*) \end{aligned} \quad (\text{S10})$$

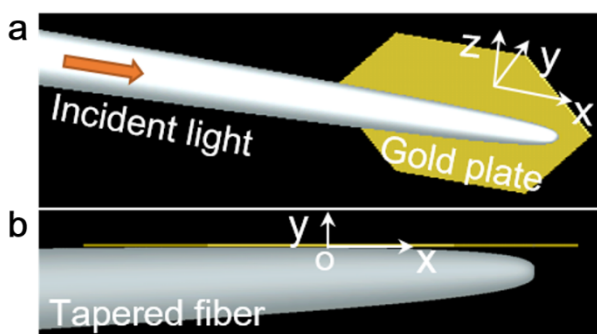
$$\begin{aligned}\langle f_y \rangle = & \frac{\epsilon_0}{4} \frac{\partial}{\partial y} \left( |E_y|^2 - |E_x|^2 - |E_z|^2 \right) + \frac{\mu_0}{4} \frac{\partial}{\partial y} \left( |H_y|^2 - |H_x|^2 - |H_z|^2 \right) \\ & + \frac{\epsilon_0}{2} \frac{\partial}{\partial x} \operatorname{Re}(E_x E_y^*) + \frac{\mu_0}{2} \frac{\partial}{\partial x} \operatorname{Re}(H_x H_y^*) + \frac{\epsilon_0}{2} \frac{\partial}{\partial z} \operatorname{Re}(E_y E_z^*) + \frac{\mu_0}{2} \frac{\partial}{\partial z} \operatorname{Re}(H_y H_z^*)\end{aligned}\quad (\text{S11})$$

$$\begin{aligned}\langle f_z \rangle = & \frac{\epsilon_0}{4} \frac{\partial}{\partial z} \left( |E_z|^2 - |E_y|^2 - |E_x|^2 \right) + \frac{\mu_0}{4} \frac{\partial}{\partial z} \left( |H_z|^2 - |H_y|^2 - |H_x|^2 \right) \\ & + \frac{\epsilon_0}{2} \frac{\partial}{\partial x} \operatorname{Re}(E_x E_z^*) + \frac{\mu_0}{2} \frac{\partial}{\partial x} \operatorname{Re}(H_x H_z^*) + \frac{\epsilon_0}{2} \frac{\partial}{\partial y} \operatorname{Re}(E_y E_z^*) + \frac{\mu_0}{2} \frac{\partial}{\partial y} \operatorname{Re}(H_y H_z^*)\end{aligned}\quad (\text{S12})$$

139  $\langle \dots \rangle$  denotes time average.

140 **5.2 Optical force analysis using Maxwell stress tensor decomposition method**

141 We use the decomposed Maxwell stress tensor (see above) to calculate optical force in the  
 142 tapered fiber-gold plate system. We choose a wavelength as 1,064 nm, the guided mode as  
 143 TE mode and the distance (D) between the gold plate and the tapered fiber end as 4.9  $\mu\text{m}$  to  
 144 analysis without loss of generality.



145  
 146 **Figure S6 | Schematic of the tapered fiber-gold plate system. a,** Perspective view and **b,**  
 147 XY view. The wavelength of the incident light is 1,064 nm. The guided mode is TE mode.  
 148 The distance (D) between the gold plate and the tapered fiber end is 4.9  $\mu\text{m}$ . The cone angle  
 149 of the tapered fiber is 6°. The side length and thickness of the gold plate is 5.4  $\mu\text{m}$  and 30 nm,  
 150 respectively. The electric field amplitude of the mode source is set as 1 V/m and the power of  
 151 the single wavelength light source is  $4.6 \times 10^{-15}$  W.

152 The force calculated by Maxwell stress tensor decomposition method is listed as follows:

153 **Table S1 | Optical force comes from each component of electromagnetic field.**

Components of $\langle f_x \rangle$	Volumetric integral (N)	Components of $\langle f_y \rangle$	Volumetric integral (N)
$\frac{\epsilon_0}{4} \frac{\partial}{\partial x}  E_x ^2$	$7.90 \times 10^{-27}$	$-\frac{\epsilon_0}{4} \frac{\partial}{\partial y}  E_x ^2$	$1.56 \times 10^{-26}$
$-\frac{\epsilon_0}{4} \frac{\partial}{\partial x}  E_y ^2$	$-1.58 \times 10^{-27}$	$\frac{\epsilon_0}{4} \frac{\partial}{\partial y}  E_y ^2$	$-3.45 \times 10^{-27}$
$-\frac{\epsilon_0}{4} \frac{\partial}{\partial x}  E_z ^2$	$-9.63 \times 10^{-27}$	$-\frac{\epsilon_0}{4} \frac{\partial}{\partial y}  E_z ^2$	$4.16 \times 10^{-26}$
$\frac{\mu_0}{4} \frac{\partial}{\partial x}  H_x ^2$	$1.45 \times 10^{-26}$	$-\frac{\mu_0}{4} \frac{\partial}{\partial y}  H_x ^2$	$1.35 \times 10^{-24}$
$-\frac{\mu_0}{4} \frac{\partial}{\partial x}  H_y ^2$	$-1.39 \times 10^{-26}$	$\frac{\mu_0}{4} \frac{\partial}{\partial y}  H_y ^2$	$-6.24 \times 10^{-26}$
$-\frac{\mu_0}{4} \frac{\partial}{\partial x}  H_z ^2$	$-8.41 \times 10^{-28}$	$-\frac{\mu_0}{4} \frac{\partial}{\partial y}  H_z ^2$	$2.52 \times 10^{-25}$
$\frac{\epsilon_0}{2} \frac{\partial}{\partial y} \text{Re}(E_x E_y^*)$	$4.80 \times 10^{-26}$	$\frac{\epsilon_0}{2} \frac{\partial}{\partial x} \text{Re}(E_x E_y^*)$	$3.77 \times 10^{-27}$
$\frac{\mu_0}{2} \frac{\partial}{\partial y} \text{Re}(H_x H_y^*)$	$-9.36 \times 10^{-26}$	$\frac{\mu_0}{2} \frac{\partial}{\partial x} \text{Re}(H_x H_y^*)$	$-8.36 \times 10^{-27}$
$\frac{\epsilon_0}{2} \frac{\partial}{\partial z} \text{Re}(E_x E_z^*)$	$4.47 \times 10^{-29}$	$\frac{\epsilon_0}{2} \frac{\partial}{\partial z} \text{Re}(E_y E_z^*)$	$3.21 \times 10^{-29}$
$\frac{\mu_0}{2} \frac{\partial}{\partial z} \text{Re}(H_x H_z^*)$	$4.45 \times 10^{-29}$	$\frac{\mu_0}{2} \frac{\partial}{\partial z} \text{Re}(H_y H_z^*)$	$-1.14 \times 10^{-28}$

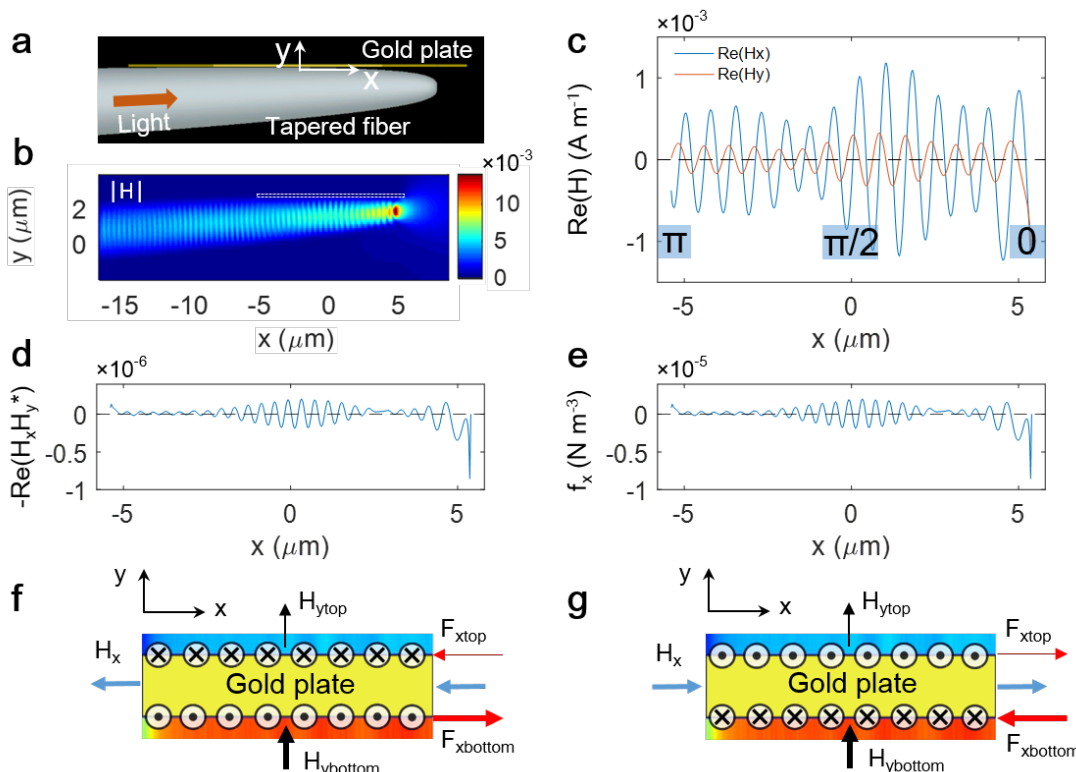
154

155 The total optical force along the tapered fiber  $F_x$  is  $-4.9 \times 10^{-26}$  N, which mainly originates  
 156 from the component  $\frac{\mu_0}{2} \frac{\partial}{\partial y} \text{Re}(H_x H_y^*)$ , of which the volumetric integral with a volume  
 157 enclosing the gold plate is  $-9.35 \times 10^{-26}$  N, as shown in Table S1. So it is a right way to focus  
 158 on magnetic field component  $H_x$  and  $H_y$  distribution when we explore the mechanism of the  
 159 pulling force in the tapered fiber-gold plate system.

160 **5.3 Optical pulling force comes from the phase difference shift (from  $\pi$  to 0) of the**  
 161 **magnetic components ( $H_x$  and  $H_y$ ) at the tapered fiber end**

162 We find that the optical force along the light propagation ( $F_x$ ) mainly comes from the

163 gradient of  $\text{Re}(H_x \times H_y)$  in the direction (y axis) perpendicular to the light propagation (see  
 164 above). It is also verified by the result that the distribution of force density  $f_x$  in Fig. S7e is  
 165 consistent with the distribution of  $-\text{Re}(H_x \times H_y)$  in Fig. S7d since there is a large negative  
 166 gradient of the field in the inner surface (the surface near the fiber) of the gold plate. Further,  
 167 we can focus on the distribution of magnetic components  $H_x$  and  $H_y$ . The phase difference of  
 168 magnetic components  $H_x$  and  $H_y$  in Fig. S7c changes from  $\pi$  at the leading edge to  $\pi/2$  in the  
 169 central section and then to 0 at the end of the gold plate. With the help of surface current  
 170 element analysis in Fig. S7f-g, we can conclude that it will be a total pulling force when the  
 171 phase difference of  $H_x$  and  $H_y$  is 0 and a total pushing force for  $\pi$ . The optical pulling force in  
 172 the tapered fiber-gold plate system comes from the phase difference shift (from  $\pi$  to 0) of the  
 173 magnetic components ( $H_x$  and  $H_y$ ) at the tapered fiber end.



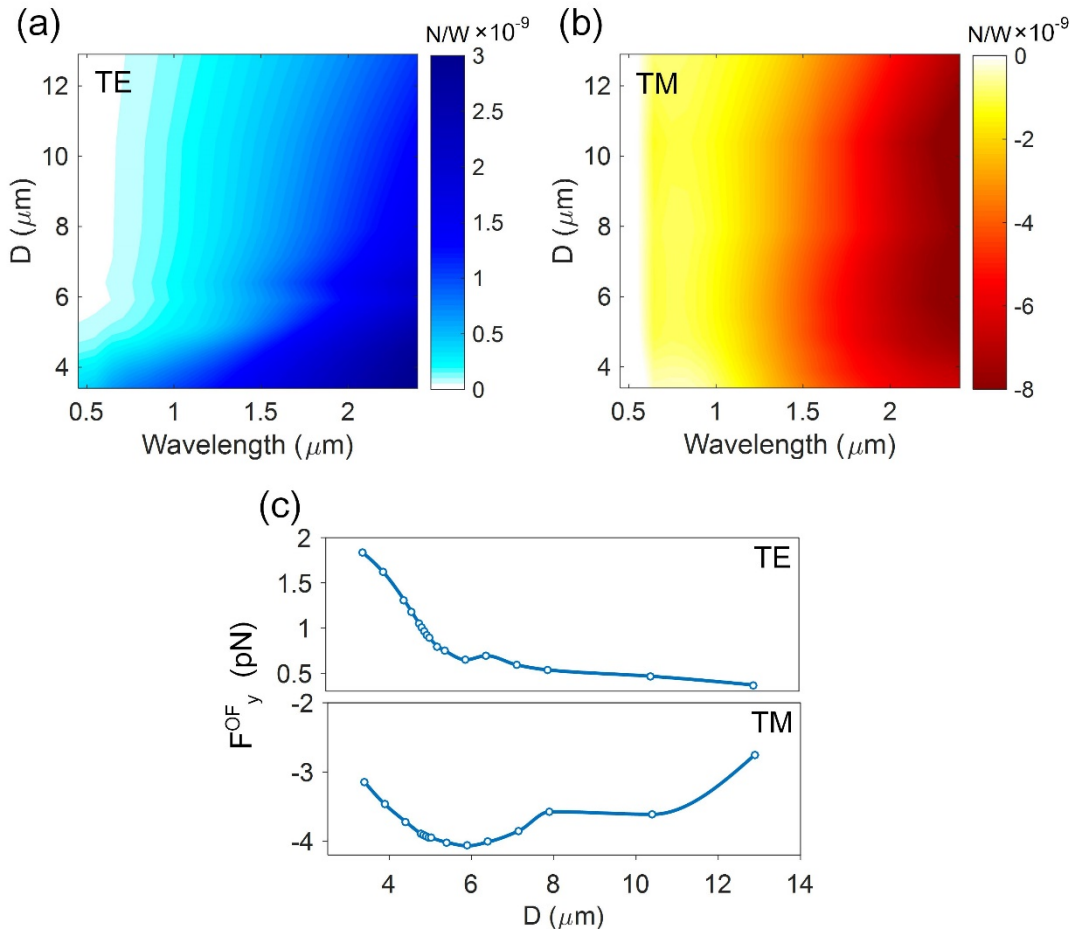
175 **Figure S7 | Phase difference shift of magnetic field components at the tapered fiber end**  
 176 **induces the pulling force for TE mode.** a, Schematic of tapered fiber-gold plate system (XY

view). The parameters in simulation is the same with that of Fig. S6 and the calculated optical force  $F_x$  is a pulling force of  $-4.9 \times 10^{-26}$  N. **b**, Magnetic field distribution. The white dashed box indicates the location of the gold plate. **c-e**, Distribution of magnetic field components  $H_x$  and  $H_y$  (**c**),  $-\text{Re}(H_x \times H_y)$  (**d**), optical force density  $f_x$  (**e**) in the bottom surface (the surface near the fiber) of the gold plate. The phase difference of magnetic components  $H_x$  and  $H_y$  in **c** changes from  $\pi$  at the leading edge to  $\pi/2$  in the central section and then to 0 at the end of the gold plate. **f-g**, Schematic of mechanism of optical pushing force and optical pulling force using surface current element analysis. The blue, black and red arrows indicate the magnetic component  $H_x$ ,  $H_y$ , and induced optical force  $F_x$  respectively. The linewidth of the arrow represents magnitude. The crosses and dots denote induced surface current elements. The phase difference of magnetic components  $H_x$  and  $H_y$  is 0 in **g** (and  $\pi$  in **f**). The induced surface currents on the bottom and top surface of the gold plate are in opposite directions, which produce larger pulling force  $F_{xin}$  and negligible pushing force  $F_{xout}$  in **g** (and larger pushing force  $F_{xin}$  and negligible pulling force  $F_{xout}$  in **f**) for the larger magnetic field in the bottom surface. Total optical force, which is  $F_{xtotal} = F_{xtop} + F_{xbottom}$ , is negative in **g** (and positive in **f**).

## 193    6 Optical force perpendicular to the gold plate surface

194    The optical force in y direction (the direction perpendicular to the surface of the gold plate) is  
195    completely different for TE mode and TM mode. It is a repulsive force ( $F_{y}^{\text{OF}} > 0$ ) for TE  
196    mode and an attractive force ( $F_{y}^{\text{OF}} < 0$ ) for transvers magnetic (TM) mode. Generally  
197    speaking, the evanescent wave of the waveguide leads to an attractive force for dielectric

198 particles or small metallic particles near the waveguide for both TE mode and TM mode.  
 199 However, for large metallic particles it is an attractive force for TM mode and a repulsive  
 200 force for TE mode. This result has been confirmed by S. Gaugiran in experiment [11].



201  
 202 **Figure S8 | Optical force in y direction.** (a, b) Calculated optical force perpendicular to the  
 203 gold plate surface ( $F_{OFy}$ ) with respect to the wavelength of light source and the distance (D)  
 204 between the center of gold plate and the tapered fiber end for (a) TE mode and (b) TM mode.  
 205 (c) Calculated optical force  $F_{OFy}$  acting on the gold plate for the supercontinuum light.

## 206 7 Force analysis from gold plate movements in experiment

207 Here, the mass of the gold plate can be calculated according the parameters of the gold plate

208 (side length, 5.4  $\mu\text{m}$ ; thickness, 30 nm; density, 19.3  $\text{g}/\text{cm}^3$ ) as follows:

209

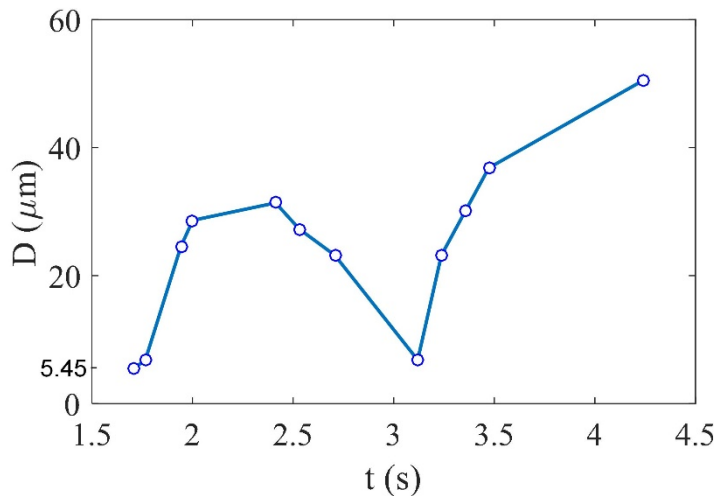
$$V = S \cdot d = \frac{3\sqrt{3}}{4} R^2 \cdot d = \frac{3\sqrt{3}}{4} 5.4^2 \cdot 0.03 \mu\text{m}^3 = 11.364 \mu\text{m}^3$$
$$m = \rho V = 19.3 \text{g}/\text{cm}^3 \times 11.364 \mu\text{m}^3 = 2.193 \times 10^{-13} \text{kg}$$

210 Then we can estimate the force acting on the gold plate in the direction of light propagation  
211 according to the average speed of the backward moving of the gold plate as follows (take the  
212 case in Supplementary Video 2 for example):

213

$$\bar{v} = at \Rightarrow a = \frac{-40 \mu\text{m}/\text{s}}{2s} = -20 \mu\text{m}/\text{s}^2$$
$$F = ma = -2.193 \times 10^{-13} \text{kg} \times 20 \mu\text{m}/\text{s}^2 = -4.39 \times 10^{-18} \text{N}$$

214 From the results, total force (including light-induced force, component of gravity force and  
215 friction force) in the direction of light propagation acting on the gold plate is in the order of  
216  $10^{-18}$  N. And the calculated optical force and photophoretic force is in the order of  $10^{-14}\sim10^{-12}$   
217 N. The light-induced force should be large enough to realize this forward and backward  
218 moving of the gold plate in the configuration. We can also infer that the friction force  
219 between the gold plate and the tapered fiber is in the order of  $10^{-14}\sim10^{-12}$  N.



220

221 **Figure S9 | Position of the gold plate on the tapered fiber changes with time.** The  
 222 distance between the center of the gold plate and the tapered fiber end is D. The position of  
 223 the gold plate is extracted from Supplementary Video 1. The average velocity of  
 224 back-forward-back movement can be calculated as:  $v_{b1} = \frac{27.27 \mu m}{0.765 s} = 35.60 \mu m/s$ ,  $v_{f1} =$   
 225  $\frac{21.82 \mu m}{0.765 s} = 28.52 \mu m/s$ ,  $v_{b2} = \frac{43.64 \mu m}{1.176 s} = 37.11 \mu m/s$ . The oscillating angular frequency can be  
 226 estimated as about 0.5 Hz if the gold plate keeps this back-forward-back movement.

227 **References**

- 228 [1] L. Tong, R. R. Gattass, J. B. Ashcom, S. He, J. Lou, M. Shen, I. Maxwell, and E. Mazur,  
 229 Nature **426**, 816-819 (2003).
- 230 [2] Z. Guo, Y. Zhang, Y. DuanMu, L. Xu, S. Xie, and N. Gu, Colloids Surf., A **278**, 33-38  
 231 (2006).
- 232 [3] L. Novotny, and B. Hecht, *Principles of nano-optics*, Ch. 13 (Academic, Cambridge,  
 233 2012).
- 234 [4] K. Wang, E. Schonbrun, and K. B. Crozier, Nano Lett. **9**, 2623–2629 (2009).
- 235 [5] C. Min, Z. Shen, J. Shen, Y. Zhang, H. Fang, G. Yuan, L. Du, S. Zhu, T. Lei, and X. Yuan,

- 236 Nat. Commun. **4**, 2891 (2013).
- 237 [6] X. Chen, Y. T. Chen, M. Yan, and M. Qiu, ACS Nano **6**, 2550-2557 (2012).
- 238 [7] D. Wolfe, A. Larraza, and A. Garcia, Phys. Fluids **28**, 037103 (2016)
- 239 [8] Scandurra, M, arXiv preprint physics/0402011 (2004).
- 240 [9] M. Scandurra, F. Iacopetti, and P. Colona, Phys. Rev. E **75**, 026308 (2007).
- 241 [10] Yinshun Wang, *Fundamental elements of applied superconductivity in electrical*  
242 *engineering*, Ch. 9 (John Wiley & Sons, 2013).
- 243 [11] S. Gaugiran, S. Gétin, J. M. Fedeli and J. Derouard, Opt. Express, **15**, 8146-8156 (2007).